Groundwater as a source of dissolved organic matter to coastal waters: Insights from radon and CDOM observations in twelve shallow coastal systems

Jackie R Webb[1, 2, 3]; Isaac R. Santos[1, 2*]; Damien T. Maher[1,4]; Douglas R Tait[1,4]; Tyler Cyronak[5]; Mahmood Sadat-Noori[1,2]; Paul Macklin[1,2]; Luke C. Jeffrey[1,2]

[1] National Marine Science Centre, Southern Cross University, Coffs Harbour, NSW 2450, Australia

[2] School of Environment, Science and Engineering, Southern Cross University, PO Box 157, Lismore, NSW 2480, Australia

[3] Department of Biology, University of Regina, Regina, SK, S4S0A2, Canada

[4] Southern Cross Geoscience, Southern Cross University, PO Box 157, Lismore, NSW 2480, Australia

[5] Scripps Institution of Oceanography, University of California San Diego, 9500 Gilman Drive, La Jolla, California, 92093, United States of America

*Corresponding author: isaac.santos@scu.edu.au Phone: +61 418 894 929

Institutional emails:

Jackie Webb: Jackie.Webb@uregina.ca

Isaac R. Santos: isaac.santos@scu.edu.au

Damien T. Maher: Damien.maher@scu.edu.au

Douglas Tait: douglas.tait@scu.edu.au

Tyler Cyronak: tcyronak@ucsd.edu

Mahmood Sadat-Noori: m.sadat-noori@unsw.edu.au

Paul Macklin: p.macklin.12@student.scu.edu.au

Luke C. Jeffrey: l.jeffrey.10@student.scu.edu.au

Abstract - The influence of groundwater discharge on dissolved organic matter (DOM) dynamics in coastal surface waters remains poorly understood. Here, we combine bottom up (i.e., groundwater-derived flux estimates) and top down (i.e., water column response) evidence to assess whether groundwater drives DOM dynamics in shallow coastal waters. We rely on automated chromophoric DOM (CDOM, a proxy for DOM) and radon (^{222}Rn; natural groundwater tracer) measurements over tidal and diel time scales in twelve shallow coastal systems, including tidal freshwater wetlands, estuaries, mangroves, coral reefs, coastal lakes, a saltmarsh, and a residential canal estate. Groundwater-derived DOC fluxes ranged from 2±2 mmol m^{-2} d^{-1} in a coral reef to a maximum of 1941±1325 mmol m^{-2} d^{-1} in a mangrove tidal creek. These groundwater fluxes replaced surface water DOC inventories on time scales ranging from ~0.5 days to several weeks. Systems with short replacement times displayed significant positive correlations between radon and CDOM in surface waters. Groundwater discharge diluted surface water DOC in four systems. Using multiple lines of evidence, we interpreted groundwater to be an important source of DOM to surface waters in four out of the twelve systems, including an offshore coral reef lagoon with very low surface water DOC and CDOM concentrations. Groundwater discharge was a negligible source of DOM in systems with high surface water DOC and CDOM concentrations such as tidal freshwater wetlands and coastal lakes. This investigation highlights the high variability in groundwater-derived DOC fluxes and responses in the water column, and demonstrates that submarine groundwater discharge and advective porewater exchange should be considered in coastal carbon budgets.

Key words: carbon cycle; fluorescent dissolved organic matter; coastal wetlands; fluorescence; FDOM.

1. Introduction

Dissolved organic matter (DOM) represents the largest marine reservoir of reduced carbon, containing two orders of magnitude greater carbon than marine biomass (Hansell et al. 2009). DOM dynamics in the coastal ocean is often related to surface water riverine inputs (Chen et al. 2007; Kowalczuk et al. 2010; Yamashita et al. 2013), with wetlands being a major source of terrestrial DOM to rivers and estuaries (Cawley et al. 2014; Huang et al. 2012). Groundwater discharge has generally been overlooked in carbon budgets of coastal aquatic systems (Moore 2010; Santos et al. 2015). However, concentrations of dissolved organic carbon (DOC) have been shown to be usually greater in groundwater than coastal surface coastal waters in spite of high variability driven by residence times, redox conditions, and carbon sources and transformations (Kim et al. 2012; Linkhorst et al. 2017; Seidel et al. 2014; Sirois et al. 2018). Local estimates of groundwater-derived DOC to coastal waters have ranged from 20% to over 100% of nearby river inputs (Goni and Gardner 2003; Sadat-Noori et al. 2016; Stewart et al. 2015). Despite increasing evidence, the influence of groundwater-surface water connectivity on aquatic carbon cycling remains relatively unconstrained.

Assessing the contribution of groundwater to coastal carbon budgets can be challenging. Radon (^{222}Rn) has been used as a natural groundwater and porewater tracer in environments ranging from inland waters to the coastal ocean (Burnett and Dulaiova 2003; Cook et al. 2003). Radon is the daughter of radium (^{226}Ra), has a half life of 3.8 days and is a noble gas. The conservative properties of ^{222}Rn, as well as its concentrated presence in groundwater compared to surface waters, make it an ideal natural tracer for groundwater input into surface waters. Continuous measurements of ^{222}Rn are now possible with automated techniques which work particularly well in capturing the groundwater exchange in dynamic tidal systems (Dulaiova et al. 2005; Stieglitz et al. 2010). Radon automation allows

78 for effective integration to other high resolution water sampling techniques to gain a more
79 complete understanding of the functioning of aquatic systems.
80 The advent of in situ optical sensors has contributed enhanced knowledge of DOM
81 dynamics in coastal waters (Jaffé et al. 2008). The use of in situ optical fluorescence sensors
82 allows for the measurement of potentially rapid changes in chromophoric dissolved organic
83 matter (CDOM), a measure of the light absorbing fraction of DOC. Reliable high resolution
84 CDOM observations over short time series have been achieved in numerous studies
85 (Saraceno et al. 2009; Spencer et al. 2007; Suryaputra et al. 2015) even though discrete
86 samples are required to obtain more specific insight into DOM sources and composition
87 (Couturier et al. 2016; Kim and Kim 2017). Given the usually strong positive relationship
88 between DOC and CDOM (Blough and Del Vecchio 2002; Kowalczuk et al. 2010; Spencer
89 et al. 2010), the use of CDOM as a proxy for DOC may alleviate some of the challenges
90 associated with more difficult DOC discrete sampling and analysis, and allow for higher
91 resolution spatiotemporal measurements.
92 In this paper, we hypothesize that groundwater is a major source of DOM to coastal
93 surface waters. This hypothesis was tested qualitatively and quantitatively in twelve diverse
94 coastal systems using groundwater and surface water observations. Firstly, we rely on
95 previously published radon mass balance models (see Table 1) to estimate DOC fluxes to
96 surface waters. Secondly, we use automated CDOM and radon time series observations over
97 at least one diel cycle to identify a potential response of groundwater inputs in surface waters.
98 These two approaches provide bottom up (i.e., groundwater fluxes to surface waters) and top
99 down (i.e., a response in surface waters) evidence to develop our hypothesis.
100
101 **2. Material and Methods**
102

Eleven diverse coastal systems along the east coast of Australia and one in the Cook Islands were investigated (Figure 1; Table 1). The systems included two tidal freshwater wetlands, two estuaries, two mangrove tidal creeks, one saltmarsh, two coral reef lagoons, two coastal lakes, and a residential canal estate. Table 1 gives a description of all study site locations and key references where further details about each study site can be obtained. All of the CDOM and most of the DOC data presented here are original. However, most of the radon and ancillary data as well as groundwater discharge estimates have been published elsewhere in different contexts (see Table 1 for data sources).

The experimental strategy at each system consisted of (1) automated, continuous observations of radon, CDOM, and ancillary parameters over at least 24 hours to assess whether groundwater inputs could create a CDOM response in surface waters (i.e., a top down response); (2) sampling groundwater near the seepage face to characterize the DOC concentrations entering surface waters; and (3) episodic sampling of DOC in surface waters.

Automated ^{222}Rn measurements were taken in surface waters over at least 24 hours at each site using a radon in air monitor (RAD7, Durridge) adapted to measure ^{222}Rn in water (Burnett et al. 2001). Surface water was continuously pumped at ~3 L min^{-1} into a gas equilibration device (GED) and the air was circulated through a closed loop system comprising of a GED, desiccant (Drierite), and ^{222}Rn-in-air monitor. Radon measurements were logged on time steps that ranged from 30 min to 1 hour, and solubility was calculated using in situ temperature and salinity (Schubert et al. 2012). Equilibration response time for ^{222}Rn using the described system and a showerhead GED was estimated to be about 30 min (Dimova et al. 2009). Therefore, a 30 min offset was applied to all radon data. Ancillary parameters including depth, salinity, and dissolved oxygen were taken concurrently using multi-parameter water quality sondes (Hydrolab MS5 and DS5X).

CDOM and chlorophyll a were measured using an *in situ* fluorescence sensor (ECO 3- Triplet, *WET Labs, Inc*.) with single excitation and emission pair of 370/460 nm and 470/695 nm, respectively. The CDOM concentration range for the sensor was 0.18 - 375 ppb, with a sensitivity of 0.18 ppb (quinine equivalents). The sensor uses UV light-emitting diodes to excite particles and silicon photodiodes to measure the emitted light over specific wavelengths. Instrument calibration was done by the manufacturer using quinine dihydrate. A drift <1% in CDOM concentrations was detected between the first and last experiment. No drift corrections were applied to the data due to the broad range in concentrations observed compared to the identified drift. The CDOM sensor collected data at time steps ranging from 1 min to 1 hour. While the automated sensor used here is ideal for time series observations and can provide high temporal resolution and large datasets, it cannot resolve the contribution of the multiple components and sources of DOM that require discrete samples and specific laboratory analysis to cover different wavelengths (Kim and Kim 2017; McKnight et al. 2001).

DOC samples were taken from surface waters at each site. The DOC sampling rate was quite variable among sites, ranging from two samples (Coastal Lake 2) to 29 samples (Estuary 1) collected hourly over the time series deployment. All DOC samples were filtered through disposable 0.7 μm Whatman GF/F syringe filters and preserved with $HgCl_2$. DOC concentrations (±4%) were determined using a continuous flow-wet chemical oxidation-method (CF-WCO-IRMS, model Aurora 1030) (St-Jean 2003).

Between 3 and 40 groundwater samples were taken at each site from shallow bores located near the assumed seepage face usually at low tide. Each bore was purged dry at least three times, and groundwater samples taken using a peristaltic pump. DOM concentrations and speciation in coastal groundwater and subterranean estuaries are driven by a number of factors including residence times and sources of carbon to the aquifer (Couturier et al. 2016;

Seidel et al. 2014). Our sampling approach was not designed to resolve DOM sources and transformation processes in the subterranean estuary. We opted for collecting groundwater samples close to the surface water body near the seepage face. Therefore, our samples represent the groundwater discharge endmember after biogeochemical transformations may have taken place within the coastal aquifer (Santos et al. 2012).

A radon mass balance model was developed for each system relying primarily on the 24-hour time series observations and groundwater observations. While different models were required for each system based on the specific morphology, the general approach was the same at all sites. Briefly, all models quantified all known sources (molecular diffusion from sediments, dissolved ^{226}Ra decay, and groundwater) and sinks (decay, atmospheric evasion, and mixing or exports) of radon in surface waters. The missing source of ^{222}Rn was assumed to be due to groundwater discharge. The contribution of dissolved ^{226}Ra decay was estimated from the average of at least two ^{226}Ra samples collected from each site and processed using a RaDeCC (Peterson et al. 2009; Waska et al. 2008). Atmospheric evasion was estimated as a function of wind speeds and currents (wetland, creek, and estuary sites) using well established equations (Burnett and Dulaiova 2003). The radon mass balance approach results in uncertainties ranging from 20% to over 100% with typical uncertainties around 50% (Sadat-Noori et al. 2015). Uncertainties in the radon-derived groundwater discharge rate were also propagated to groundwater DOC fluxes using the standard deviation of all DOC groundwater samples.

3. Results

Eleven out of the twelve shallow coastal systems investigated displayed dynamic tidal trends in CDOM concentrations. During ebb tides, an increase in CDOM was observed in

most systems, while a decrease in CDOM was seen at flood tide (Figures 2 and 3). However, Wetlands 1 and 2 had the opposite trend with higher CDOM concentrations during the flood tides. Coastal Lake 1 was non-tidal and displayed a diel CDOM cycle. As expected, estuaries, mangroves and wetlands had the highest CDOM concentrations, while the lowest concentrations were observed in coral reefs (Table 2). Salinity trends closely followed tides in most systems. In Mangrove 1, an increase in salinity concurrent with low tides implies evapotranspiration and no freshwater inputs. In Mangrove 2 and the two estuaries, a drop in salinity at low tide indicates some drainage of upstream freshwater. Radon also followed a tidal trend in all systems but the non-tidal Coastal Lake 1. In several cases, especially Estuary 1 and Mangrove 2, the ^{222}Rn peak lagged the low tide by 1-3 hours.

Significant positive correlations (p<0.01) between CDOM and the groundwater tracer ^{222}Rn were observed in eight of the twelve systems investigated (Figure 4). Negative correlations were observed in both Tidal Wetlands and in Coral Reef 2, and no correlations were observed in Coastal Lake 1. Mangrove 2 and Estuary 1 had noticeable hysteresis patterns in which CDOM increased rapidly at relatively low ^{222}Rn followed by a drop in CDOM at peak ^{222}Rn concentrations. A plot of average CDOM concentrations against average salinity values from all systems excluding Tidal Wetland 2 (Rocky Mouth Creek; unique in that the pH was ~4) revealed that CDOM decreased along with increasing salinity gradient as expected (Figure 5). Variability in the mid-salinity range was highly influenced by Estuary 1 (Korogoro Creek) that had the widest salinity range during our observations (Figure 2). CDOM in surface waters also correlated to DOC across multiple systems with the two lake systems plotting as outliers (Figure 5).

Groundwater samples (Table 2) had consistent low oxygen with average dissolved oxygen saturation ranging between 3% and 26% in Canal Estate and Coastal Lake 1, respectively. Groundwater temperatures ranged between 20 and 26 °C at all systems, except

for the temperate Saltmarsh with an average temperature of 15 °C. DOC concentrations in groundwater ranged from 83 μmol L^{-1} in Coral Reef 2 to >2300 μmol L^{-1} around the Canal Estate and Mangrove 2. In five systems (Estuary 1, Tidal Wetlands 1 and 2, Coastal Lakes 1 and 2) DOC concentrations in surface waters exceeded groundwater concentrations, implying that groundwater exchange would dilute surface water concentrations, negating our initial hypothesis. In the other seven systems, DOC concentrations in groundwater samples were on average 5-fold greater than surface water samples, demonstrating the potential for groundwater to act as a source of DOC to surface waters.

Radon mass balance models were used to estimate groundwater discharge rates into surface waters. Because most of the radon data has been published elsewhere (see Table 1), here we simply describe the estimated groundwater discharge rates and related DOC fluxes (Table 2). The estimated groundwater discharge rates varied over two orders of magnitude from 0.1 cm d^{-1} in the non-tidal Coastal Lake 2 (Jeffrey et al. 2016) to 35 cm d^{-1} in Estuary 1 (Sadat-Noori et al. 2015). Multiplying the groundwater discharge rates by the average groundwater DOC concentrations in each system resulted in groundwater-derived DOC fluxes ranging over three orders of magnitude from 2±2 to 1941±1325 mmol m^{-2} d^{-1}.

4. Discussion

We combine bottom up (i.e., groundwater fluxes) and top down (i.e., a response in the water column) evidence to assess whether groundwater may be an important source of DOM to surface waters into the twelve systems under investigation. Combining bottom up and top down evidence builds confidence when interpreting the biogeochemical response of surface waters to groundwater discharge (Robinson et al. 2018). Even large groundwater sources may be minor relative to other local sources of DOM (such as surface runoff), so the absolute flux

227 estimates need to be put in perspective. Positive correlations between CDOM and radon may
228 be driven by simple mixing and would alone offer tenuous evidence for groundwater as a
229 source of DOM. Insights into the relative contribution of groundwater to the overall DOM
230 pool were obtained by estimating the replacement time of the DOC inventories, i.e., how long
231 it would take for groundwater-derived DOC to replace the surface water pool. To conclude
232 that groundwater is an important source of DOM to surface waters, we required that all lines
233 of evidence converge to the same interpretation. A summary of the evidence available for
234 each system is shown in Figure 7. Each evidence becomes meaningful only when interpreted
235 in light of the other lines of evidence.

236 Our investigation extends the range of previously reported groundwater-derived DOC
237 fluxes to a minimum of 2±2 mmol m^2 d^{-1} in Coral Reef 2 to a maximum of 1941±1325 mmol
238 m^2 d^{-1} in Mangrove 2 with an overall average of 374±557 mmol m^2 d^{-1}. In a recent summary
239 of the literature, Sadat-Noori (2016) described groundwater-derived DOC fluxes in nine
240 systems to range from 20 to 170 mmol m^2 d^{-1}. These estimates were used to suggest
241 groundwater discharge to be a major source of DOM to surface waters after comparisons to
242 nearby river inputs (Moore et al. 2006; Porubsky et al. 2014; Santos et al. 2012). The lowest
243 DOC fluxes summarized by Sadat-Noori et al. (2016) were found off sandy beaches such as a
244 the West coast of Florida (USA; Santos et al. 2008) and Moreton Bay (Australia; Stewart et
245 al. 2015), while the highest fluxes were found in the saltmarsh-dominated Okatee Estuary
246 (Moore et al. 2006).

247 Putting our estimated groundwater-derived DOC fluxes in perspective of other DOC
248 sources in coastal waters is difficult. The groundwater-derived DOC fluxes presented here are
249 usually one order of magnitude greater than DOC diffusive fluxes at the sediment-water
250 interface estimated from benthic chamber and sediment core incubations. DOC fluxes at the
251 sediment interface have been estimated to be 0.6 mmol m^2 d^{-1} in continental shelf sediments,

252 2.3 mmol m^2 d^{-1} in estuaries, 27.3 mmol m^2 d^{-1} in saltmarshes, and 34.3 mmol m^2 d^{-1} in
253 mangroves (Maher and Eyre 2010 and references therein). Therefore, overlooking
254 groundwater-derived DOC fluxes may underestimate a potentially important role of
255 sediments and aquifers in coastal DOM budgets. We highlight, however, that additional work
256 would be needed to define the spatial extent of groundwater fluxes that are likely to be higher
257 near the shoreline (Burnett et al. 2006; Taniguchi et al. 2003), while diffusive fluxes may
258 occur over larger areas.

259 The large variability in CDOM concentration over the tidal and diel cycles implies
260 that the timescale of the source is comparable to the timescale of CDOM losses via mixing as
261 previously observed in tidal systems (Bowers and Brett 2008). To further put our results in
262 perspective, we use the surface water DOC inventory to define how long it would take for
263 groundwater inputs to replace the local surface water DOC pool. All shallow coastal systems
264 investigated here, except for the two coastal lakes, were well flushed with most of the surface
265 water drained over a diurnal cycle (i.e., two semi-diurnal tidal cycles). DOC inventories
266 ranged from 43 mmol m^{-2} in Coral Reef 2 to >1500 mmol m^{-2} in the two Tidal freshwater
267 wetlands. Dividing the DOC inventories by the groundwater-derived DOC fluxes yielded
268 replacement times ranging from <12 hours (i.e., one tidal cycle) in Coral Reef 1, Mangrove 2,
269 and Canal Estate, up to weeks in the two Coastal Lakes, two Tidal Wetlands, and Coral Reef
270 2.

271 Systems with a short DOC replacement time could be interpreted to have groundwater
272 as a major source of DOM. If this was the case, we would also expect significant positive
273 correlations between radon (groundwater discharge proxy; Burnett and Dulaiova 2003;
274 Stieglitz 2005) and CDOM (DOM proxy; Kowalczuk et al. 2010; Spencer et al. 2010) in
275 surface waters with a short DOC replacement time. Indeed, all the systems with estimated
276 DOC replacement times <2 days had significant positive correlations (Figure 7). However, a

277 close inspection of the data revealed that both Mangrove 2 and Estuary 1 exhibited hysteresis
278 loops in the CDOM versus ^{222}Rn relationship (Figure 4), preventing the use of a linear
279 regression model to describe these data. In both cases, the CDOM peak coincided with an
280 initial salinity drop (Figure 2). Therefore, we interpret the hysteresis as evidence for an initial
281 delivery of surface fresh waters enriched in DOM followed by groundwater inputs as would
282 be expected for systems with upstream wetlands storing freshwater (Santos and Eyre 2011).
283 The hysteresis patterns highlights that a simple correlation analysis alone should not be used
284 to deduce a cause-effect relationship.

285 Salinity scatter plots are often used to interpret DOM production and consumption in
286 estuarine waters (Blough and Del Vecchio 2002). However, because of the narrow salinity
287 variability in most systems (Figures 2 and 3), this approach cannot be applied here. Estuary 1
288 was the only system with a broad salinity range and a clear concave shape in the CDOM
289 versus salinity relationship (Figure 5) that can be interpreted as an estuarine DOM source
290 (Blough and Del Vecchio 2002; Suryaputra et al. 2015). Since groundwater DOC was lower
291 than surface water DOC (Table 2) in Estuary 1, groundwater discharge is unlikely to be a
292 major source of DOC, highlighting that multiple lines of evidence are important when
293 interpreting our results. Estuary 1 is surrounded by wetlands that can release DOC to surface
294 waters (Cawley et al. 2014; Huang et al. 2012). We suggest that wetland inputs explain the
295 concave shape in the CDOM vs. salinity scatter, the higher concentrations of DOC in surface
296 water than groundwater, and the hysteresis patterns in the radon vs. CDOM scatter plot.

297 CDOM concentrations within Tidal Wetland 2 were uncharacteristically low for
298 freshwater wetlands. Tidal Wetland 2 had the lowest pH out of all the waters, ranging from 3-
299 5 during the diel cycle (Figure 3). Inhibition of DOM photo-oxidation under acidic conditions
300 can cause variation in the fluorescence intensity of dissolved organic matter (Patel-Sorrentino
301 et al. 2002; Vodacek 1992). Contrastingly, lowering of the pH may cause a decrease in

CDOM concentrations as a result of naturally occurring iron accelerating photo-oxidation of CDOM (Gao and Zepp 1998). Extensive drainage of the upstream acid sulfate soil wetlands drive low surface water pH (Santos and Eyre 2011) and high levels of iron monosulfide (Bush et al. 2004) within this creek. Fe-accelerated photo-oxidation or DOM co-precipitation with iron flocs may explain low CDOM concentrations within Tidal Wetland 2. Alternatively, the input of humic CDOM may potentially explain the decrease in pH as observed in a boreal coastal aquifer where detailed DOM analysis revealed a large contribution of lignin-type organic compounds (Couturier et al. 2016). Unfortunately, the automated florescence sensor used here cannot provide insight into the speciation and sources of DOM and how it relates to pH.

We also considered a diurnal (rather than tidal) CDOM trend as evidence for photomineralization cycles. The non-tidal Coastal Lake 1 was the only system with an obvious diel cycle. Photomineralization of DOM caused by exposure to UV radiation can drive short term changes in CDOM concentrations within lake systems (Bertilsson and Tranvik 2000; Moran et al. 2000). In surface waters, up to 75% of DOM absorbance loss by natural sunlight can occur on time scales as short as 28 days (Opsahl and Benner 1998). Photomineralization can account for a large loss in DOM from aquatic systems, as was found in a black water swamp where a 46% removal of terrigenous DOM was observed through this pathway (Obernosterer and Benner 2004). In the non-tidal Coastal Lake 1, the observed 3% drop in CDOM during the day was potentially related to UV driven photomineralization, and would remove the lake CDOM pool within ~36 days. An increase in CDOM during the night and decrease during the day was similar to the diurnal variability previously observed within a river system (Spencer et al. 2007), but was not apparent in the eleven tidal-dominated systems.

Coral Reef 1 (Heron Island) had detailed CDOM time series data available for groundwater. Groundwater ^{222}Rn and CDOM concentrations taken from a beach bore on Heron Island agreed well with the values predicted from the projection of the CDOM versus ^{222}Rn regression during the surface water time series (Figure 6). Heron Island is a small offshore coral cay reef with highly permeable coarse carbonate sands and no river inputs. A tidal range of about 2 m creates steep hydraulic gradients which drives seawater recirculation in and out of island sediments (McMahon and Santos 2017). Furthermore, the natural variability of ^{222}Rn and CDOM had similar ranges over a diel cycle (CDOM=27%, ^{222}Rn=26%). Combined with the high groundwater-derived DOC fluxes, these observations provide evidence that groundwater is the dominant source of CDOM to Coral Reef 1, and suggest that where surface water runoff is minimal, groundwater can exert a major control over CDOM dynamics. Therefore, the lack of other major DOM sources and the low inventories of DOM in surface waters allow for groundwater discharge to play a major role in DOM dynamics in Coral Reef 1.

In summary, this paper reports groundwater-derived DOC fluxes to twelve coastal systems and investigates whether these fluxes may create a detectable response in surface waters. DOC was enriched (>2-fold) in groundwater relative to surface waters in six out of the twelve systems. This enrichment generated a groundwater-derived DOC flux ranging from 2±2 to 1941±1325 mmol m^{-2} d^{-1}. Those highly variable DOC fluxes created a detectable response in surface waters in four systems (Canal Estate, Saltmarsh, Coral Reef 1, and Estuary 2). Groundwater discharge as traced by radon had minor influence on surface water DOM in the Tidal Wetlands, Coastal Lakes, and Coral Reef 2, with ambiguous interpretation in the other systems.

Our results combined with earlier estimates of groundwater-derived DOC fluxes (e.g., Goni and Gardner 2003; Moore et al. 2011; Stewart et al. 2015) illustrate the highly variable

nature of groundwater DOC fluxes, surface water CDOM dynamics, and groundwater DOC concentrations in coastal environments. Except for a minor contribution of groundwater in wetland-dominated systems, there was no consistent patterns within individual ecosystem types. The importance of groundwater as a source of DOM to coastal waters is likely to be influenced by the surrounding terrestrial environment and hydrological regime. In environments such as wetlands that produce a strong signal of DOM in surface waters (Mulholland 2003), the contribution of groundwater-derived DOM will likely be masked. Coastal systems that experience distinct fluctuations in surface water movement (tidal pumping) often support higher rates of groundwater exchange, and will increase the potential for groundwater to be a source of DOM. While we cannot generalize our findings due to short-term datasets and limited replication of ecosystems, our observations in a diverse array of shallow coastal waters demonstrate that groundwater can potentially be important in some cases and should be considered when developing coastal carbon budgets. Coupling automated radon and automated CDOM observations may provide a reasonable, simple approach to assess linkages between groundwater discharge and DOM dynamics even though correlations between radon and CDOM did not necessarily represent a cause-effect relationship.

Acknowledgements. Field observations and analytical instrumentation were funded by the Australian Research Council (DP120101645, LP100200732, DP110103638, DE140101733, and LE120100156). We acknowledge the multiple students and staff members from the School of Environment, Science and Engineering for valuable contribution to data collection.

References

Bertilsson, S., and L. J. Tranvik. 2000. Photochemical transformation of dissolved organic matter in lakes. Limnology and Oceanography **45:** 753-762.

Blough, N., and R. Del Vecchio. 2002. Chromophoric DOM in the coastal environment, p. 509-546. *In* D. A. Hansell and C. A. Carlson [eds.], Biogeochemistry of Marine Dissolved Organic Matter. Academic Press.

Bowers, D. G., and H. L. Brett. 2008. The relationship between CDOM and salinity in estuaries: An analytical and graphical solution. Journal of Marine Systems **73:** 1-7.

Burnett, W. C. and others 2006. Quantifying submarine groundwater discharge in the coastal zone via multiple methods. Science of the Total Environment **367:** 498-543.

Burnett, W. C., and H. Dulaiova. 2003. Estimating the dynamics of groundwater input into the coastal zone via continuous radon-222 measurements. Journal of Environmental Radioactivity **69:** 21-35.

Burnett, W. C., G. Kim, and D. Lane-Smith. 2001. A continuous monitor for assessment of ^{222}Rn in the coastal ocean. Journal of Radioanalytical and Nuclear Chemistry **249:** 167-172.

Bush, R. T., L. A. Sullivan, D. Fyfe, and S. Johnston. 2004. Redistribution of monosulfidic black oozes by floodwaters in a coastal acid sulfate soil floodplain. Australian Journal of Soil Research **42:** 603-607.

Cawley, K., Y. Yamashita, N. Maie, and R. Jaffé. 2014. Using optical properties to quantify fringe mangrove inputs to the dissolved organic matter (DOM) pool in a subtropical estuary. Estuaries and Coasts **37:** 399-410.

Chen, Z., C. Hu, R. N. Conmy, F. Muller-Karger, and P. Swarzenski. 2007. Colored dissolved organic matter in Tampa Bay, Florida. Marine Chemistry **104:** 98-109.

Cook, P. G., G. Favreau, J. C. Dighton, and S. Tickell. 2003. Determining natural groundwater influx to a tropical river using radon, chlorofluorocarbons and ionic environmental tracers. Journal of Hydrology **277:** 74-88.

Couturier, M., C. Nozais, and G. Chaillou. 2016. Microtidal subterranean estuaries as a source of fresh terrestrial dissolved organic matter to the coastal ocean. Marine Chemistry **186:** 46-57.

Cyronak, T., I. R. Santos, D. V. Erler, D. T. Maher, and B. D. Eyre. 2014. Drivers of pCO_2 variability in two contrasting coral reef lagoons: The influence of submarine groundwater discharge. Global Biogeochemical Cycles**:** 2013GB004598.

Dimova, N., W. C. Burnett, and D. Lane-Smith. 2009. Improved automated analysis of radon (Rn-222) and thoron (Rn-220) in natural waters. Environmental Science & Technology **43:** 8599-8603.

Dulaiova, H., R. Peterson, W. Burnett, and D. Lane-Smith. 2005. A multi-detector continuous monitor for assessment of ^{222}Rn in the coastal ocean. Journal of Radioanalytical and Nuclear Chemistry **263:** 361-365.

Gao, H., and R. G. Zepp. 1998. Factors influencing photoreactions of dissolved organic matter in a coastal river of the Southeastern United States. Environmental Science & Technology **32:** 2940-2946.

Gatland, J. R., I. R. Santos, D. T. Maher, T. M. Duncan, and D. V. Erler. 2014. Carbon dioxide and methane emissions from an artificially drained coastal wetland during a flood: Implications for wetland global warming potential. Journal of Geophysical Research **119:** 1698–1716, doi:1610.1002/2013JG002544.

Gleeson, J., I. R. Santos, D. T. Maher, and L. Golsby-Smith. 2013. Groundwater–surface water exchange in a mangrove tidal creek: Evidence from natural geochemical tracers and implications for nutrient budgets. Marine Chemistry **156:** 27-37.

Goni, M. A., and L. R. Gardner. 2003. Seasonal dynamics in dissolved organic carbon concentrations in a coastal water-table aquifer at the forest-marsh interface. Aquatic Geochemistry **9:** 209-232.

Hansell, D. A., C. A. Carlson, D. J. Repeta, and R. Schlitzer. 2009. Dissolved organic matter in the ocean: A controversy stimulates new insights. Oceanography **22:** 202-211.

Huang, T.-H., Y.-H. Fu, P.-Y. Pan, and C.-T. A. Chen. 2012. Fluvial carbon fluxes in tropical rivers. Current Opinion in Environmental Sustainability **4:** 162-169.

Jaffé, R., D. McKnight, N. Maie, R. Cory, W. H. McDowell, and J. L. Campbell. 2008. Spatial and temporal variations in DOM composition in ecosystems: The importance of long-term monitoring of optical properties. Journal of Geophysical Research: Biogeosciences **113:** G04032.

Jeffrey, L. C., D. T. Maher, I. R. Santos, A. McMahon, and D. R. Tait. 2016. Groundwater, acid and carbon dioxide dynamics along a coastal wetland, lake and estuary continuum. Estuaries and Coasts **39:** 1325-1344.

Kim, J., and G. Kim. 2017. Inputs of humic fluorescent dissolved organic matter via submarine groundwater discharge to coastal waters off a volcanic island (Jeju, Korea). Scientific Reports **7:** 7921.

Kim, T.-H., H. Waska, E. Kwon, I. G. N. Suryaputra, and G. Kim. 2012. Production, degradation, and flux of dissolved organic matter in the subterranean estuary of a large tidal flat. Marine Chemistry **142–144:** 1-10.

Kowalczuk, P., M. Zablocka, S. Sagan, and K. Kulinski. 2010. Fluorescence measured in situ as a proxy of CDOM absorption and DOC concentration in the Baltic Sea. Oceanologia **52:** 431-471.

Linkhorst, A., T. Dittmar, and H. Waska. 2017. Molecular Fractionation of Dissolved Organic Matter in a Shallow Subterranean Estuary: The Role of the Iron Curtain. Environmental Science & Technology **51:** 1312-1320.

Maher, D., and B. D. Eyre. 2010. Benthic fluxes of dissolved organic carbon in three temperate Australian estuaries: Implications for global estimates of benthic DOC fluxes. Journal of Geophysical Research **115:** G04039.

Maher, D. T., I. R. Santos, L. Golsby-Smith, J. Gleeson, and B. D. Eyre. 2013. Groundwater-derived dissolved inorganic and organic carbon exports from a mangrove tidal creek: The missing mangrove carbon sink? Limnology and Oceanography **58:** 475-488.

McKnight, D. M., E. W. Boyer, P. K. Westerhoff, P. T. Doran, T. Kulbe, and D. T. Andersen. 2001. Spectrofluorometric characterization of dissolved organic matter for indication of precursor organic material and aromaticity. Limnology and Oceanography **46:** 38-48.

McMahon, A., and I. R. Santos. 2017. Nitrogen enrichment and speciation in a coral reef lagoon driven by groundwater inputs of bird guano. Journal of Geophysical Research: Oceans **122:** 7218-7236.

Moore, W. S. 2010. The effect of submarine groundwater discharge on the ocean. Annual Review of Marine Science **2:** 59-88.

Moore, W. S. and others 2011. Radium-based pore water fluxes of silica, alkalinity, manganese, DOC, and uranium: A decade of studies in the German Wadden Sea. Geochimica et Cosmochimica Acta **75:** 6535-6555.

Moore, W. S., J. O. Blanton, and S. B. Joye. 2006. Estimates of flushing times, submarine groundwater discharge, and nutrient fluxes to Okatee Estuary, South Carolina. Journal of Geophysical Research **111:** C09006, doi:09010.01029/02005JC003041.

Moran, M. A., W. M. Sheldon, and R. G. Zepp. 2000. Carbon loss and optical property changes during long-term photochemical and biological degradation of estuarine dissolved organic matter. Limnology and Oceanography **45:** 1254-1264.

Mulholland, P. J. 2003. 6 - Large-Scale Patterns in Dissolved Organic Carbon Concentration, Flux, and Sources A2 - Findlay, Stuart E.G, p. 139-159. *In* R. L. Sinsabaugh [ed.], Aquatic Ecosystems. Academic Press.

Obernosterer, I., and R. Benner. 2004. Competition between biological and photochemical processes in the mineralization of dissolved organic carbon. Limnology and Oceanography **49:** 117-124.

Opsahl, S., and R. Benner. 1998. Photochemical reactivity of dissolved lignin in river and ocean waters. Limnology and Oceanography **43:** 1297-1304.

Patel-Sorrentino, N., S. Mounier, and J. Y. Benaim. 2002. Excitation–emission fluorescence matrix to study pH influence on organic matter fluorescence in the Amazon basin rivers. Water Research **36:** 2571-2581.

Perkins, A. K., I. R. Santos, M. Sadat-Noori, J. R. Gatland, and D. T. Maher. 2015. Groundwater seepage as a driver of CO_2 evasion in a coastal lake (Lake Ainsworth, NSW, Australia). Environmental Earth Sciences**:** 1-14.

Peterson, R. N., W. C. Burnett, N. Dimova, and I. R. Santos. 2009. Comparison of measurement methods for radium-226 on manganese-fiber. Limnology and Oceanography: Methods **7:** 196-205.

Porubsky, W. P., N. B. Weston, W. S. Moore, C. Ruppel, and S. B. Joye. 2014. Dynamics of submarine groundwater discharge and associated fluxes of dissolved nutrients, carbon, and trace gases to the coastal zone (Okatee River estuary, South Carolina). Geochimica et Cosmochimica Acta **131:** 81-97.

Robinson, C. E., P. Xin, I. R. Santos, M. A. Charette, L. Li, and D. A. Barry. 2018. Groundwater dynamics in subterranean estuaries of coastal unconfined aquifers: Controls on submarine groundwater discharge and chemical inputs to the ocean. Advances in Water Resources **in press**.

Sadat-Noori, M., D. T. Maher, and I. R. Santos. 2016. Groundwater Discharge as a Source of Dissolved Carbon and Greenhouse Gases in a Subtropical Estuary. Estuaries and Coasts **39:** 639-656.

Sadat-Noori, M., I. R. Santos, C. J. Sanders, L. M. Sanders, and D. T. Maher. 2015. Groundwater discharge into an estuary using spatially distributed radon time series and radium isotopes. Journal of Hydrology **528:** 703-719.

Santos, I. R. and others 2015. Porewater exchange as a driver of carbon dynamics across a terrestrial-marine transect: Insights from coupled ^{222}Rn and pCO_2 observations in the German Wadden Sea. Marine Chemistry **171:** 10-20.

Santos, I. R., W. Burnett, J. P. Chanton, B. Mwashote, I. G. N. A. Suryaputra, and T. Dittmar. 2008. Nutrient biogeochemistry in a Gulf of Mexico subterranean estuary and groundwater-derived fluxes to the coastal ocean. Limnology and Oceanography **53:** 705-718.

Santos, I. R., P. L. M. Cook, L. Rogers, J. de Weys, and B. D. Eyre. 2012. The 'salt wedge pump': Convection-driven porewater exchange as a source of dissolved organic and inorganic carbon and nitrogen to an estuary. Limnology and Oceanography **57:** 1415-1426.

Santos, I. R., and B. D. Eyre. 2011. Radon tracing of groundwater discharge into an Australian estuary surrounded by coastal acid sulphate soils. Journal of Hydrology **396:** 246-257.

Saraceno, J. F., B. A. Pellerin, B. D. Downing, E. Boss, P. A. M. Bachand, and B. A. Bergamaschi. 2009. High-frequency in situ optical measurements during a storm event: Assessing relationships between dissolved organic matter, sediment concentrations, and hydrologic processes. Journal of Geophysical Research: Biogeosciences **114:** G00F09.

Schubert, M., A. Paschke, E. Lieberman, and W. C. Burnett. 2012. Air−water partitioning of ^{222}Rn and its dependence on water temperature and salinity. Environmental Science & Technology **46:** 3905-3911.

Seidel, M. and others 2014. Biogeochemistry of dissolved organic matter in an anoxic intertidal creek bank. Geochimica et Cosmochimica Acta **140:** 418-434.

Sippo, J. Z., D. T. Maher, D. R. Tait, S. Ruiz-Halpern, C. J. Sanders, and I. R. Santos. 2017. Mangrove outwelling is a significant source of oceanic exchangeable organic carbon. Limnology and Oceanography Letters **2:** 1-8.

Sirois, M., M. Couturier, A. Barber, Y. Gélinas, and G. Chaillou. 2018. Interactions between iron and organic carbon in a sandy beach subterranean estuary. Marine Chemistry **202:** 86-96.

Spencer, R. G. M. and others 2010. Temporal controls on dissolved organic matter and lignin biogeochemistry in a pristine tropical river, Democratic Republic of Congo. Journal of Geophysical Research: Biogeosciences **115:** G03013.

Spencer, R. G. M. and others 2007. Diurnal variability in riverine dissolved organic matter composition determined by in situ optical measurement in the San Joaquin River (California, USA). Hydrological Processes **21:** 3181-3189.

St-Jean, G. 2003. Automated quantitative and isotopic (^{13}C) analysis of dissolved inorganic carbon and dissolved organic carbon in continuous-flow using a total organic carbon analyser. Rapid Communications in Mass Spectrometry **17:** 419-428.

Stewart, B. T., I. R. Santos, D. Tait, P. A. Macklin, and D. T. Maher. 2015. Submarine groundwater discharge and associated fluxes of alkalinity and dissolved carbon into Moreton Bay (Australia) estimated via radium isotopes. Marine Chemistry **174:** 1-12.

Stieglitz, T. 2005. Submarine groundwater discharge into the near-shore zone of the Great Barrier Reef, Australia. Marine Pollution Bulletin **51:** 51-59.

Stieglitz, T. C., P. G. Cook, and W. C. Burnett. 2010. Inferring coastal processes from regional-scale mapping of ^{222}Radon and salinity: examples from the Great Barrier Reef, Australia. Journal of Environmental Radioactivity **101:** 544-552.

Suryaputra, I. G. N. A., I. R. Santos, M. Huettel, W. C. Burnett, and T. Dittmar. 2015. Non-conservative behavior of fluorescent dissolved organic matter (FDOM) within a subterranean estuary. Continental Shelf Research **110:** 183-190.

Tait, D. R., D. T. Maher, P. A. Macklin, and I. R. Santos. 2016. Mangrove pore water exchange across a latitudinal gradient. Geophysical Research Letters**:** 2016GL068289.

Taniguchi, M. and others 2003. Spatial and temporal distributions of submarine groundwater discharge rates obtained from various types of seepage meters at a site in the Northeastern Gulf of Mexico. Biogeochemistry **66:** 35-53.

Vodacek, A. 1992. An explanation of the spectral variation in freshwater CDOM fluorescence. Limnology and Oceanography **37:** 1808-1813.

Waska, H., S. Kim, G. Kim, R. N. Peterson, and W. C. Burnett. 2008. An efficient and simple method for measuring ^{226}Ra using the scintillation cell in a delayed coincidence counting system (RaDeCC). Journal of Environmental Radioactivity **99:** 1859-1862.

Yamashita, Y., J. N. Boyer, and R. Jaffé. 2013. Evaluating the distribution of terrestrial dissolved organic matter in a complex coastal ecosystem using fluorescence spectroscopy. Continental Shelf Research **66:** 136-144.

Figure 1: Satellite images showing the location of the twelve study sites. Coordinates and site descriptions are found in Table 1. White circle shows the location of the surface water time series station. Groundwater samples were taken from the shoreline near the surface water time series station.

Figure 2: Time series data for six systems over a full diel cycle showing CDOM and ancillary parameters. Shading represents dark hours.

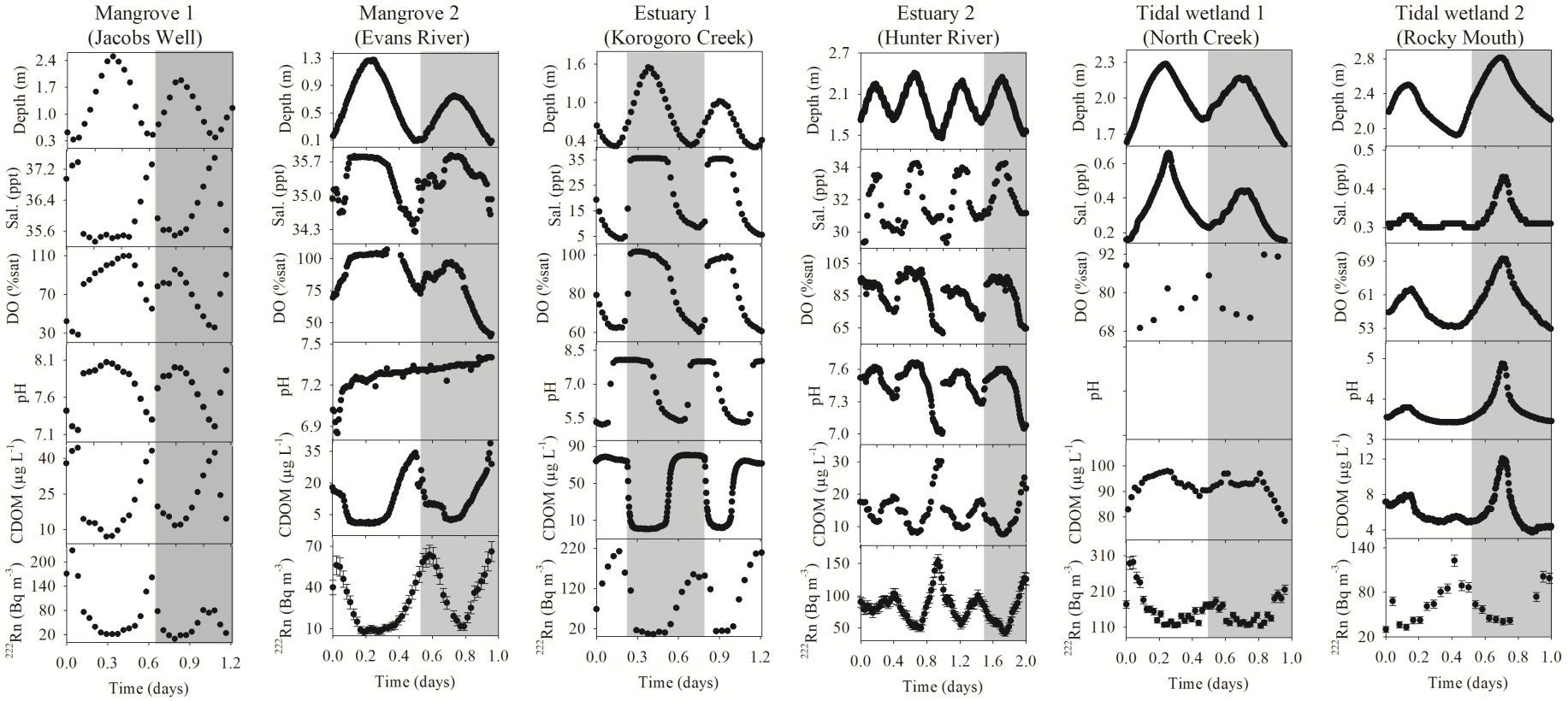

Figure 3: Time series data for six systems over a full diel cycle showing CDOM and ancillary parameters. Shading represents dark hours.

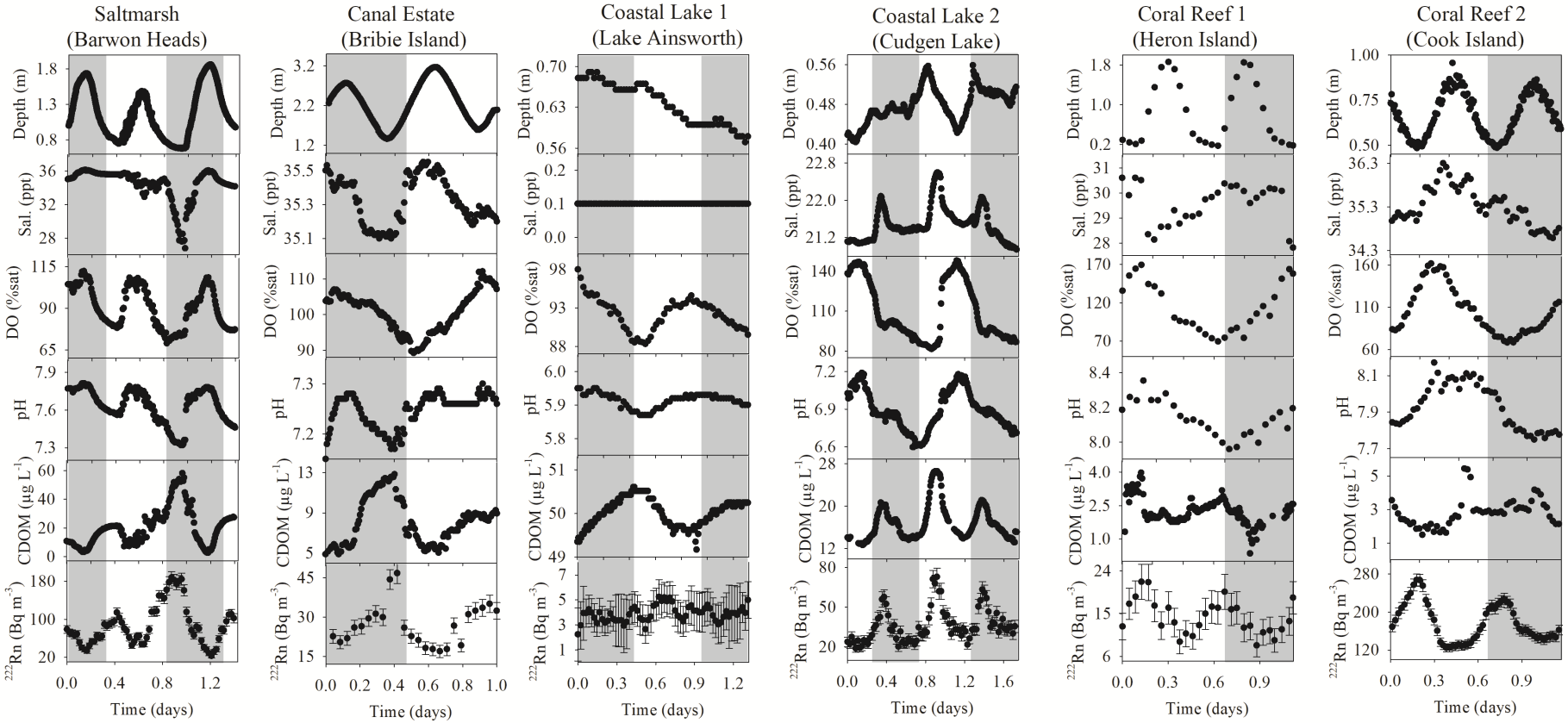

Figure 4: Surface water CDOM versus ^{222}Rn concentrations at the twelve different coastal systems. Relationships were assessed using a linear regression model. Lines are plotted only when correlations were considered significant at $p<0.001$, and when a false positive relationship was not apparent as in the cases of Mangrove 2 and Estuary 1.

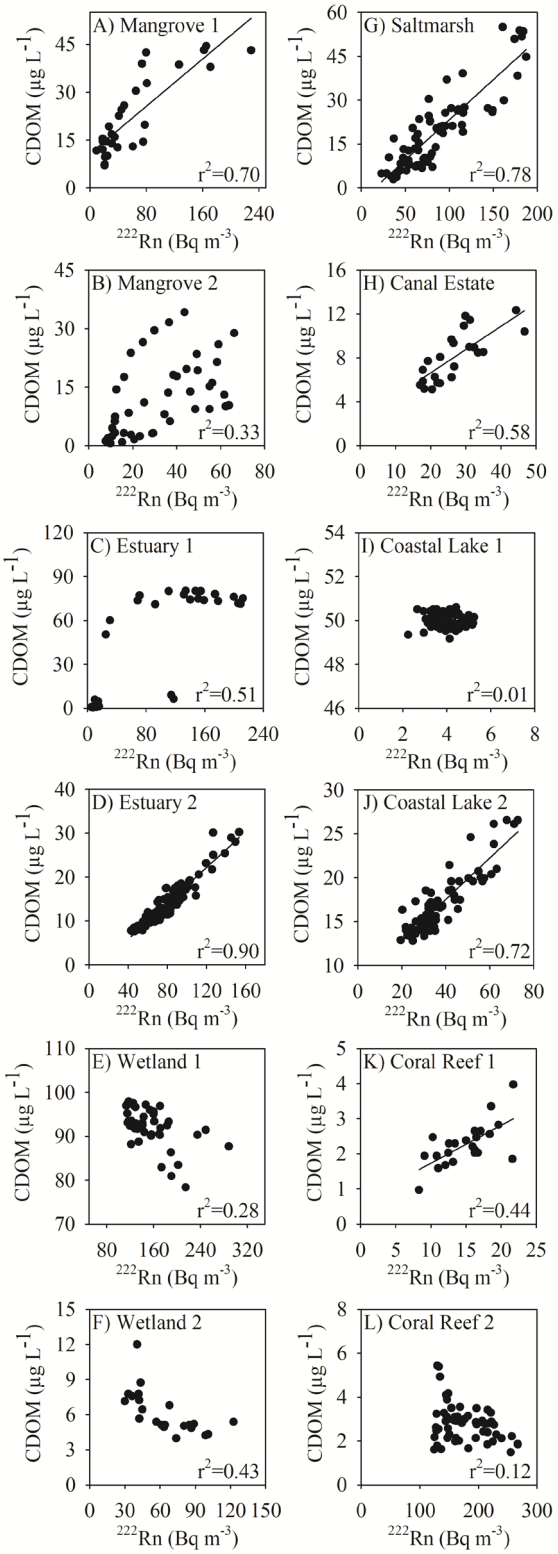

Figure 5: CDOM concentrations as a function of salinity (left) and DOC (right) for all systems. Large open circles represent the average for each system, while small grey circles represent individual observations. Estuary 1 was the only system with a wide range in salinity values over a tidal cycle, revealing an estuarine source with a concave distribution. The system names on the bottom left of the salinity plot appear in order of high to low CDOM.

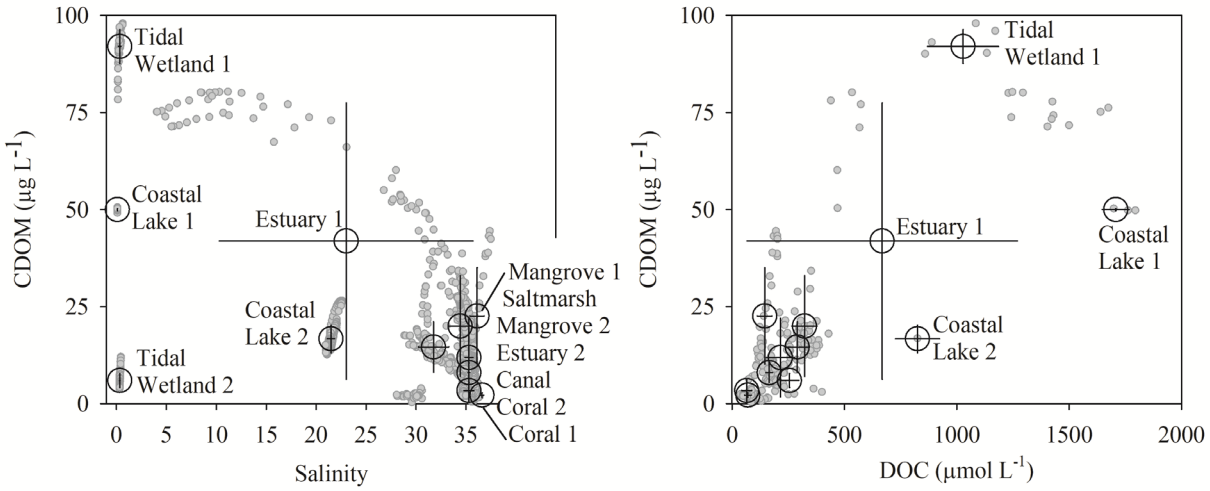

Figure 6: Heron Island correlation between CDOM (µg L^{-1}) and ^{222}Rn (Bq m^{-3}) for surface water (black) and groundwater (white) showing 95% confidence intervals. The projection of the surface water regression intercepts the groundwater observations, providing evidence for groundwater discharge as a major local source of CDOM. The inset zooms in surface water observations.

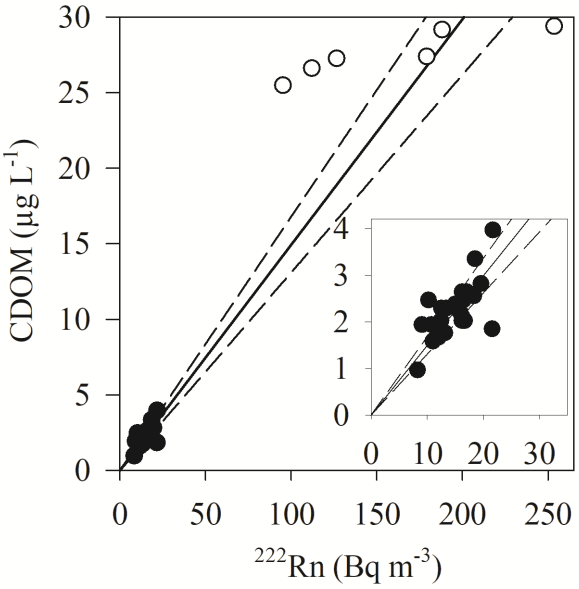

Figure 7: Summary of evidence used to interpret whether groundwater is an important source of DOM to surface waters. White bars indicate when groundwater can be interpreted as a source, and black when not.

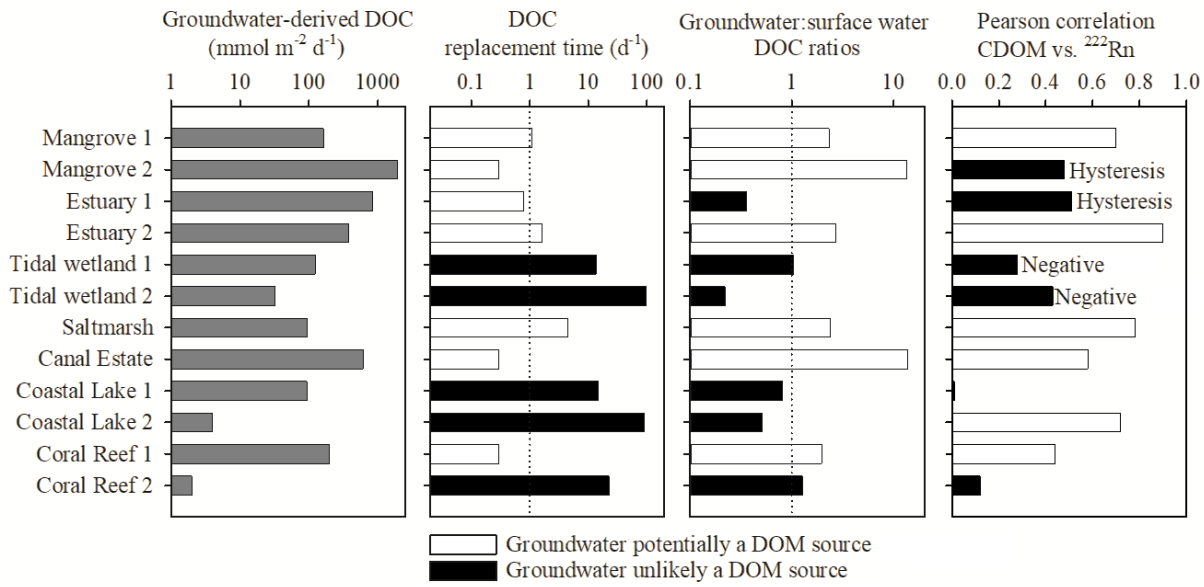

Table 1: General study site information, sampling period and duration, and source of data. All the CDOM and most of the DOC data are original. Most of the radon and ancillary data have been published elsewhere.

Site	Location	Coordinates	Site description	Source of data	Start date and time	Duration
Mangrove 1	Jacobs Well, Australia	27.78043°S 153.3810°E	Tidal saltwater creek surrounded by mangroves	^{222}Rn, DO, and salinity (Gleeson et al. 2013) and DOC (Maher et al. 2013)	11/1/2012 04:30	29 h
Mangrove 2	Evans River, Australia	29.12099°S 153.4280°E	Tidal creek surrounded by mangrove and saltmarsh	Unpublished	10/10/2013 07:04	25 h
Estuary 1	Korogoro Creek, Australia	31.05778°S 153.0562°E	Small estuary draining a wetland/dunes	^{222}Rn, DO, DOC, and salinity (Sadat-Noori et al. 2015)	78/6/2013 12:00	29 h
Estuary 2	Hunter River, Australia	32.85001°S 151.7670°E	Tidal creek draining to an estuary surrounded by mangroves	^{222}Rn, DO, and salinity (Tait et al. 2016) and DOC (Sippo et al. 2017)	15/11/2014 0:00	48 h
Tidal wetland 1	North Creek, Australia	28.78844°S 153.5638°E	Tidal freshwater creek downstream of drained acid sulphate soils	Unpublished	22/07/2011 09:00	24 h
Tidal wetland 2	Rocky Mouth Creek, Australia	29.09610°S 153.3262°E	Tidal freshwater creek draining acid sulphate soils and sugar cane	^{222}Rn, DO, salinity, and DOC (Gatland et al. 2014)	27/5/2013 08:45	25 h
Salt marsh	Barwon Heads, Australia	38.26210°S 144.4960°E	Tidal creek surrounded by saltmarsh and mangrove	^{222}Rn, DO, and salinity (Tait et al. 2016) and DOC (Sippo et al. 2017)	23/11/2014 23:20	34 h
Canal Estate	Bribie Island, Australia	27.04909°S 153.1430°E	Residential canal estate waters in a sandy island with pine trees	Unpublished	26/11/2012 18:30	24 h
Coastal Lake 1	Lake Ainsworth, Australia	28.7818°S 153.5846°E	Freshwater dunal lake with frequent cyanobacterial blooms	^{222}Rn, DO, and salinity (Perkins et al. 2015)	8/12/2013 20:00	32 h
Coastal Lake 2	Cudgen Lake, Australia	28.3162°S 153.5647°E	Coastal lake downstream of acid sulphate soil wetlands	^{222}Rn, DO, and salinity (Jeffrey et al. 2016)	17/12/2015 12:30	41 h
Coral 1	Heron Island, Australia	23.4435°S 151.9129°E	Healthy coral reef lagoon near a coral cay island	^{222}Rn, DO, and salinity (Cyronak et al. 2014)	9/10/2011 12:00	27 h
Coral 2	Raratonga, Cook Islands	21.26445°S 159.73466°E	Impacted coral lagoon near a volcanic island	^{222}Rn, DO, and salinity (Cyronak et al. 2014)	17/03/2012 07:00	28 h

Table 2: Summary of groundwater observations in the twelve coastal systems (average ± standard deviation). Most of the groundwater radon, ancillary data, and groundwater discharge rate estimates have been published elsewhere (see Table 1).

	Sample size	Salinity	DO (% sat.)	CDOM ($\mu g\ L^{-1}$)	^{222}Rn ($Bq\ m^{-3}$)	DOC ($\mu mol\ L^{-1}$)	Groundwater discharge ($cm\ d^{-1}$)	Groundwater-derived DOC ($mmol\ m^{-2}\ d^{-1}$)
Mangrove 1	6	27.6 ± 5.9	12 ± 4	52 ± 13	702 ± 242	338 ± 119	8.4 ± 1.8	162 ± 67
Mangrove 2	6	18.8 ± 8.1	25 ± 20	99 ± 49	542 ± 204	2873 ± 528	7.3 ± 4.8	1941 ± 1325
Estuary 1	48	21.5 ± 6.2	13 ± 18	n/a	467 ± 346	242 ± 82	35.0 ± 12.0	847 ± 408
Estuary 2	12	35.1 ± 6.6	6 ± 4	45 ± 6	1258 ± 779	791 ± 175	14.7 ± 2.9	736 ± 218
Tidal Wetland 1	10	0.5 ± 0.6	19 ± 10	25 ± 16	1376 ± 1077	872 ± 841	38.9 ± 12.2	124 ± 126
Tidal Wetland 2	5	1.2 ± 0.1	5 ± 1	43 ± 11	865 ± 425	290 ± 47	1.1 ± 1.5	32 ± 44
Saltmarsh	12	35.3 ± 4.4	11 ± 14	40 0 10	1617 ± 823	766 0 208	3.7 ± 2.4	164 ± 116
Canal Estate	19	1.9 ± 6.8	3 ± 5	n/a	1011 ± 987	2283 ± 2367	2.9 ± 1.3	614 ± 694
Coastal Lake 1	5	0.3 ± 0.2	n/a	96 ± 21	149 ± 12	1391 ± 230	0.7 ± 0.6	93 ± 82
Coastal Lake 2	15	0.5 ± 0.7	26 ± 21	31 ± 31	42100 ± 8833	420 ± 472	0.1 ± 0.1	4 ± 6
Coral Reef 1	7	25.0 ± 6.5	6 ± 2	28 ± 2	1099 ± 761	137 ± 46	29.7 ± 10.3	199 ± 96
Coral Reef 2	3	2.5 ± 3.0	n/a	n/a	5983 ± 2717	83 ± 23	1.1 ± 0.8	2 ± 2